Effect of Bioconvection of a Radiating Casson Hybrid Mhd Nanofluid Past Over a Thin Needle

[1]Arindam Das,
Assistant Teacher of Mathematics, Bhubanmayee Jr. High School, Pandapara Kalibari, Jalpaiguri,735132, West Bengal, India
Email: greatari111@gmail.com

[2]Dr. Annapurna Ramakrishna Sinde,
Department of Mathematics, Dr. A P J Abdul Kalam University, Indore, Madhya Pradesh - 452016
E-mail: jayabhandari15@gmail.com

[3] Dr. Md Tausif Sk,
Department of Mathematics, Acharya B N Seal College, Cooch Behar – 736101, West Bengal, India
Email: tausifdropbox@gmail.com

Article Info
Page Number: 13293 – 13298
Publication Issue:
Vol 71 No. 4 (2022)

Abstract: The photograph reactant nature of TiO2 tracks down applications in restorative field to dispense with malignant growth cells, microbes, and infections under gentle bright enlightenment and the antibacterial quality of Ag makes the arrangement Ag+TiO2 pertinent for different purposes. It can likewise be utilized in other designing machines and businesses like mugginess sensor, coolants, and in footwear industry. Thus, this study manages the examination of the impacts of attractive field and warm radiation in Casson liquid progression of electrically directing Ag+TiO2/H2O half breed nanofluid. Besides, the gyrotactic microorganisms are utilized as dynamic blenders to forestall agglomeration and sedimentation of TiO2 that happens because of its hydrophobic nature. The numerical model appears as incomplete differential conditions with consistency and warm conductivity being the elements of volume division. These conditions are switched over completely to conventional differential conditions by utilizing similitude change and are addressed by RKF-45 technique with the guide of shooting strategy. It is seen that the expansion in the size of the needle upgrades the general exhibition of the cross breed nanofluid. Moreover, the temperature of the mixture nanofluid elevates with the expansion in volume part. It is seen that the contact delivered by the Lorentz force builds the temperature of the nanofluid.

Article History
Article Received: 25 October 2022
Revised: 30 November 2022
Accepted: 15 December 2022

Keywords: thin needle, radiating hybrid nanofluid, gyrotactic microorganisms, Casson fluid, magnetic field

Introduction:

The organisms are delegated "outrageous psychrophiles" (cold adoring <0 ○C), "thermophiles" (between 50 ○C to 80 ○C), "hyperthermophiles" (between 80 ○C to 121 ○C) in light of the scope of temperature they can endure. The class of microorganisms is picked according to the necessity of the climate. Platt's report [1] was quick to talk about the term bioconvection when he noticed the "Benard cells" structure because of the development polygonal examples of Tetrahymena (e.g., ciliate, lash) in thick societies. The investigation of Ghorai and Slope [2] portrayed the example development in the microbial suspension through bioconvection.

Choi and Eastman [3] acquainted nanofluids with satisfy the requests of the business to have a liquid that has better intensity move qualities. These nanofluids are framed by suspending the nanosized metal particles into the standard liquid. Xuan and collaborators [4,5] had caused the warm scattering in the movement to expand the course of intensity transport. These examinations demonstrated that the nanofluids track down various applications in the field of industrialized cooling, assembling of cleanser, biomedical applications, atomic reactors, CPU innovation, and so forth. Sinha and Misra [6] examined the initiated attractive field on magnetohydrodynamic (MHD) stream and it was stretched out to Bio nanofluids by Basir et al. [7]. A portion of the purposes of magneto nanofluids are in MHD siphons and gas pedals, cancer therapy, therapy of hyperthermia, attractive reverberation imaging, sanitized gadgets, blockage evacuation in conduits, MHD Power generators, and so forth, Refs. [8-13].

Nanofluids have significant power in microfluidic gadgets where deficient blending was constantly an issue. Besides, the joule warming created by dynamic blenders would have harmed the bio-applications. To conquer this issue, Kuznetsov [14] supplanted the dynamic blenders by motile microorganisms for improving the blending that lead to bioconvection in nanofluids. These microorganisms settle the nanoparticles suspended in the liquid and their development causes bioconvection. It is a phenomenon initiated by the aggregate development of self-moved microorganisms. Kuznetsov expanded his review from bioconvection to thermo bioconvection [15-17]. Aziz et al. [18] concentrated on the progression of nanofluids within the sight of gyrotactic microorganisms. Tham et al. [19, 20] focused on the significance of Bioconvection in bio microsystems for microfluidic types of gear. Shaw et al. [21] saw that the intensity move of a nanofluid was profoundly impacted by Thermophoresis and Brownian movement. The examinations connected with bioconvective progression of nanofluid in permeable square pit within the sight of oxytactic microorganisms should be visible in [22] and [23]. Khan and Makinde [24, 25] examined bioconvection and noticed an expansion in the thickness of the base liquid because of the presence of microorganisms. Gireesha et al. [26, 27] examined the effect of Brownian movement and Thermophoresis on the three-layered bioconvective stream. These works roused the specialists to utilize bioconvection in bio microsystems, biomedical, and microfluidic gadgets, power modules, wastewater therapies, assembling of liquor, bread shop items, and so on.

Suspensions containing the single class nanoparticle may not have every one of the necessary qualities for a particular application. For instance, Al_2O_3 shows apparent substance dormancy and soundness yet will offer low warm conductivity. While, particles like aluminum (Al), silver (Ag), copper (Cu), and so forth, have higher warm conductivity and are unsound

and synthetically receptive. Subsequently, the blending of these nanoparticles with various physical and synthetic bonds structures nanofluid called half and half nanofluids and track down applications in atomic wellbeing, drug industry, cooling of electronic radiators, and so on. Hayat and Nadeem [28] investigated that the hybridization of the liquid expanded the pace of intensity move. Chamkha and collaborators [29, 31] examined the natural convection in the half breed nanofluid under attractive field in a square nook. Manjunatha et al. [32] talked about the progression of Cu-Al_2O_3/H_2O half breed nanofluid affected by factor thickness.

A meager layer nearby a surface to which the liquid is limited and the stream is characterized as limit layer by Ludwig Prandtl. A slim needle is an item with illustrative upheaval around which a stream remains axisymmetric and the limit layers are close to the measurement of the item. Needle with nonuniform thickness has numerous useful applications lately. Biomimetic is a significant field where such a stream is frequently examined. This incorporates blood stream in the veins, and spread of disease in the body. Other modern applications should be visible in Streamline features, assembling of estimating gear and in apparatuses where metal turning is available, for example, Wind designing, and water stream about marines. Taking into account these applications the investigation of Newtonian liquid stream around a meager needle was examined by Lee [33] [39]. Afterward, Narain and Uberoi [34, 35], [40, 41] examined the convection in the stream past a needle. The impacts of surface intensity transition and wall temperature for the stream close to nonisothermal needles were examined by Chen and Smith [42]. Ishak et al. [43] researched the free stream past a needle. This work was gone on by Ahmad et al. [44] for the investigation of helping and contradicting stream of nanofluid. Grosan and Pop [45] performed mathematical investigation for constrained convection stream of Cu/H_2O and Al_2O_3/H_2O over a non isothermal surface of a needle utilizing Tiwari-Das model. Hayat et al. [46] examined the intensity move through carbon nano tubes (CNTs) for stream around a needle by considering variable intensity transition.

$Ag+TiO_2$ is a photograph impetus utilized as an antibacterial specialist since Ag upgrades the photograph synergist action of TiO_2 under the UV radiations by diminishing the recombination pace of photograph invigorated charge transporters that improves the natural builds due to the hydroxyl revolutionaries framed by the protons [47,48]. The antibacterial action of Ag TiO_2 against E-Coli under noticeable light was read up for 0.15% silver doped titanium dioxide with 0.05% convergence of dopant showed the most noteworthy disintegration pace of Rhodamine [49]. Moreover, the plasmonic design of $Ag+TiO_2$ coordinated with optical fiber can be utilized as mugginess sensor. The axisymmetric stream of nanofluid assumes a significant part in medication and modern mechanical cycles and one of such is the stream past a slender needle. For example, in the clinical field, the vast majority of the created and delivered immunizations for human and creature assurance against sicknesses are comprised of weakened organisms in the liquid antibodies. These microbiomes of people and different creatures experience stream in numerous areas of the body, including the digestive system, stomach, urinary lot, mouth, and lungs under different temperatures. In persistent blended tank bioreactors and photograph bioreactors, microorganisms are presented to laminar and tempestuous streams produced to improve their development and bioprocesses (like aging) by guaranteeing supplement blending, gas trade, and ideal light openness. Thus, a

genuine endeavor is had to dissect the effect Attractive flied on Casson liquid progression of $Ag+TiO_2/H_2O$ half breed nanofluid through dainty needle. The uniqueness of the issue is utilization of bio-dynamic blenders to agglomeration of $Ag+TiO_2$ nanoparticles and evades the affidavit of nanoparticles.

Mathematical formulation:

Consider a two layered progression of half breed nanofluid past a slender needle of range r=R(x). The limit layer is thought to be moving with uniform speed U_w in the equivalent or inverse heading of the free stream of the uniform speed U_{in}. In the event that the surface temperature of the needle T_w is thought to be more noteworthy than the surrounding temperature T_{in} then it compares to a warmed needle and the condition $T_w < T_{in}$ relates to a cooled needle. In this review, this temperature distinction is thought to be unimportant. It is expected that the grouping of suspended nanoparticles is weaken for the counteraction of the bioconvection insecurity. The nanoparticles are suspended utilizing surfactants, with the goal that it forestalls the agglomeration and surface strain among water and nanoparticles. Water, an optically thick medium is decided to be the base liquid as it gives a climate that is the most appropriate for the consistently conveyed gyrotactic microorganisms to make due. This study expects round shape for the suspended nanoparticles.

Table 1: Properties of Nanofluid and Hybrid nanofluid:

Properties	Nanofluid	Hybrid nanofluid
Density $\left(kg.m^{-3}\right)$	$\rho_{nf}=(1-\varphi)\rho_{bf}+\varphi\rho_{np}$	$\rho_{hnf}=(1-\varphi_2)\begin{pmatrix}(1-\varphi_1)\rho_{bf}\\+\varphi_1\rho_{np1}\end{pmatrix}+\varphi_2\rho_{np2}$
Heat capacity $\left(J.kg^{-1}.\mathrm{K}^{-1}\right)$	$\left(\rho c_p\right)_{nf}=(1-\varphi)\left(\rho c_p\right)_{bf}+\varphi\left(\rho c_p\right)_{np}$	$\left(\rho c_p\right)_{hnf}=(1-\varphi_2)\begin{pmatrix}(1-\varphi_1)\left(\rho c_p\right)_{bf}\\+\varphi_1\left(\rho c_p\right)_{np1}\end{pmatrix}+\varphi_2\left(\rho c_p\right)_{np2}$
Viscosity $\left(\mathrm{N.m}^{-2}\right)$	$\mu_{nf}=\frac{\mu_{bf}}{(1-\varphi)^{2.5}}$	$\mu_{hnf}=\frac{\mu_{bf}}{(1-\varphi_1)^{2.5}(1-\varphi_2)^{2.5}}$
Thermal conductivity $\left(\mathrm{W.m}^{-1}.K^{-1}\right)$	$\frac{\kappa_{nf}}{\kappa_{bf}}=\frac{\kappa_{np}+2\kappa_{bf}-2\varphi\left(\kappa_{bf}-\kappa_{np}\right)}{\kappa_{np}+2\kappa_{bf}+\varphi\left(\kappa_{bf}-\kappa_{np}\right)}$	$\frac{\kappa_{hnf}}{\kappa_{nf}}=\frac{\kappa_{np2}+2\kappa_{nf}-2\varphi_2\left(\kappa_{nf}-\kappa_{np2}\right)}{\kappa_{np2}+2\kappa_{nf}+\varphi_2\left(\kappa_{nf}-\kappa_{np2}\right)}$, $\frac{\kappa_{nf}}{\kappa_{bf}}=\frac{\kappa_{np1}+2\kappa_{bf}-2\varphi_1\left(\kappa_{bf}-\kappa_{np1}\right)}{\kappa_{np1}+2\kappa_{bf}+\varphi_1\left(\kappa_{bf}-\kappa_{np1}\right)}$
Electrical conductivity $\left(\mathrm{S.m}^{-1}\right)$	$\frac{\sigma_{nf}}{\sigma_{bf}}=\frac{\sigma_{np}+2\sigma_{bf}-2\varphi\left(\sigma_{bf}-\sigma_{np}\right)}{\sigma_{np}+2\sigma_{bf}+\varphi\left(\sigma_{bf}-\sigma_{np}\right)}$	$\frac{\sigma_{hnf}}{\sigma_{nf}}=\frac{\sigma_{np2}+2\sigma_{bf}-2\varphi_2\left(\sigma_{bf}-\sigma_{np2}\right)}{\sigma_{np2}+2\sigma_{bf}+\varphi_2\left(\sigma_{bf}-\sigma_{np2}\right)}$, $\frac{\sigma_{nf}}{\sigma_{bf}}=\frac{\sigma_{np1}+2\sigma_{bf}-2\varphi_1\left(\sigma_{bf}-\sigma_{np1}\right)}{\sigma_{np1}+2\sigma_{bf}+\varphi_1\left(\sigma_{bf}-\sigma_{np1}\right)}$

The agglomeration of nanoparticles can be forestalled by utilizing dynamic blenders either as synthetic compounds or as microorganisms. Involving dynamic blenders as synthetic compounds is neither efficient nor keeps the machine from being harmed. Thus, the utilization of self-impelled microorganisms is liked over synthetic substances. These microorganisms are heavier than the encompassing medium where they move and they are having a tendency to swim upwards. These microorganisms answer specific boosts by swimming in a particular heading [50]. In view of this reaction, the microorganisms are delegated gravitaxis, phototaxis, magnetotaxis, chemotaxis, gyrotaxis, and so on, and the movement of these microorganisms is constrained by gravity, light, attractive field, substance species, and mass angle, separately. This study incorporates gyrotactic microorganisms that move because of the excellence of mass inclination and requires no extra power for its movement. Subsequently, involving these microorganisms as dynamic blenders is affordable and productive. The microorganism's movement in the nanofluid can be approximated as

$$m = M\mu + M\mu' - D_M \nabla M \quad (01)$$

Where $\mu' = \left(\frac{bW_c}{\Delta C}\right)\nabla C$. Here, both ∇C and changes in the centralization of the mass liquid ΔC, are viewed as in the model because of the reality these microorganisms move in the homogeneous mass liquid during bioconvection.

A magnetic field B_0 is applied opposite to the progression of the electrically leading crossover nanofluid. The connection of attractive field with the actuated current J and the Lorentz force f is characterized as

$$f = J \times B = \sigma_{hnf} B_0^2 \left(v_x - U_{in}\right) \quad (02)$$

Table 2: Thermophysical properties of base fluid and nanoparticles [47]:

	$\rho\left(kg.m^{-3}\right)$	$\sigma\left(S.m^{-1}\right)$	$\kappa\left(W.m^{-1}.K^{-1}\right)$	$c_p\left(\mathrm{J.kg^{-1}}.K^{-1}\right)$
H_2O	997.1	5.5×10^{-6}	0.6071	4179
Ag	10490	63×10^{6}	429	235
TiO_2	4250	2.4×10^{6}	8.953	686.2

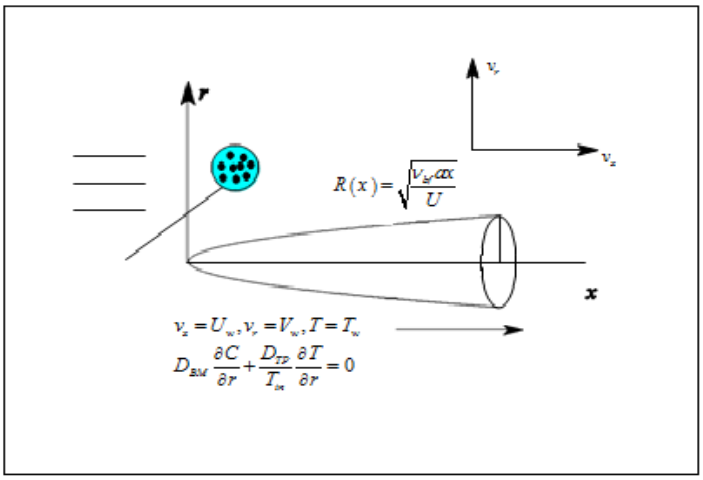

Figure 1: Physical flow model

The overseeing conditions in needle shaped are organized for the progression of crossover nanofluid past a meager needle are communicated as [38, 50]. The thermophysical properties are characterized in (Table 1) and their actual constants are yielded (Table 2)

$$\left.\begin{aligned}
&\frac{\partial}{\partial x}\left(rv_x\right)+\frac{\partial}{\partial r}\left(rv_r\right)=0\\
&v_x\frac{\partial v_x}{\partial x}+v_r\frac{\partial v_x}{\partial r}=\left(1+\frac{1}{\beta}\right)\frac{\nu_{hnf}}{r}\frac{\partial}{\partial r}\left(r\frac{\partial v_x}{\partial r}\right)-\frac{\sigma_{hnf}B_0^2}{\rho_{hnf}}\left(v_x-U_{in}\right)\\
&v_x\frac{\partial T}{\partial x}+v_r\frac{\partial T}{\partial r}=\frac{\kappa_{hnf}}{\left(\rho c_p\right)_{hnf}}\frac{1}{r}\frac{\partial}{\partial r}\left(r\frac{\partial T}{\partial r}\right)+\tau\left\{D_{BM}\frac{\partial T}{\partial r}\frac{\partial C}{\partial r}+\frac{D_{TP}}{T_{in}}\left(\frac{\partial T}{\partial r}\right)^2\right\}+\frac{1}{\left(\rho c_p\right)_{hnf}}\frac{\partial q_r}{\partial r}\\
&v_x\frac{\partial C}{\partial x}+v_r\frac{\partial C}{\partial r}=\frac{D_{BM}}{r}\frac{\partial}{\partial r}\left(r\frac{\partial C}{\partial r}\right)+\frac{D_{TP}}{T_{in}}\frac{1}{r}\frac{\partial}{\partial r}\left(r\frac{\partial T}{\partial r}\right)\\
&v_x\frac{\partial M}{\partial x}+v_r\frac{\partial M}{\partial r}=\frac{D_{MO}}{r}\frac{\partial}{\partial r}\left(r\frac{\partial M}{\partial r}\right)-\left(\frac{bW_c}{\Delta C}\right)\frac{1}{r}\frac{\partial}{\partial r}\left(M\frac{\partial C}{\partial r}\right)
\end{aligned}\right\}$$

(02)

With the appropriate boundary conditions are

$$\left.\begin{aligned}
&v_x=U_w, v_r=V_w, T=T_w, D_{BM}\frac{\partial C}{\partial r}+\frac{D_{TP}}{T_{in}}\frac{\partial T}{\partial r}=0, M=M_w \text{ at } r=R\left(x\right)\\
&v_x\to U_{in}, T\to T_{in}, C\to C_{in}, M\to M_{in} \text{ as } r\to\infty
\end{aligned}\right\}$$

(03)

The energy equation in (02) is outlined utilizing the possibility of Rosseland [51] where warm radiation is accounted. The Plank number and the optical thickness are the significant boundaries worried about the impacts of radiation on the stream and intensity move. Obviously, during the disentanglement of Rosseland estimate, these two boundaries vanish after the determination. This determination will lead to another boundary called radiation boundary as

the thorough radiation coefficient. This boundary is result of Board number and the optical thickness [52] and it is characterized as follows:

$$q_r = -\frac{4\sigma^*}{3k}\frac{\partial T^4}{\partial r} \quad (04)$$

This guess incorporates dissemination term that was presented in light of the hypothesis of preservation of energy. Since the temperature distinctions between T_w and T_∞ is thought to be essentially little, the Rosseland guess can be linearized by growing T^4 as per the Taylor series about T_{in}. The decreased development subsequent to dismissing the higher request terms is

$$T^4 = 4T_{in}^3 T - 3T_{in}^4 \quad (05)$$

By using this expression, the energy Eq. in (02) reduces to

$$v_x\frac{\partial T}{\partial x} + v_r\frac{\partial T}{\partial r} = \frac{\kappa_{hnf}}{\left(\rho c_p\right)_{hnf}}\frac{1}{r}\frac{\partial}{\partial r}\left(r\frac{\partial T}{\partial r}\right) + \tau\left\{D_{BM}\frac{\partial T}{\partial r}\frac{\partial C}{\partial r} + \frac{D_{TP}}{T_{in}}\left(\frac{\partial T}{\partial r}\right)^2\right\} + \frac{16\sigma^* T_{in}^3}{3k\left(\rho c_p\right)_{hnf}}\frac{\partial^2 T}{\partial r^2} \quad (06)$$

The following similarity transformation transforms the partial differential equations to ordinary differential equations:

$$\xi = \frac{Ur^2}{\nu_{bf}x}, \omega = \nu_{bf}xf'(\xi), U = U_w + U_{in}, \vartheta(\xi) = \frac{T - T_{in}}{T_w - T_{in}}, h(\xi) = \frac{C - C_{in}}{C_w - C_{in}}, m(\xi) = \frac{M - M_{in}}{M_w - M_{in}} \quad (07)$$

The stream capability ω is characterized as $v_x = \frac{1}{r}\frac{\partial \omega}{\partial r}$ and $v_r = -\frac{1}{r}\frac{\partial \omega}{\partial x}$, where v_x is the axial speed part and v_r is the radial speed part. If $\xi = a$ is a consistent relating to the outer layer of upset alluding to the mass of the needle then setting $\xi = a$ in Eq. (02) gives $R(x) = \sqrt{\frac{\nu_{bf}ax}{U}}$ that depicts the shape and size of the body width and its surface. The local skin friction coefficient, local Nusselt number, local Sherwood number and local microorganism number are defined as

$$\left.\begin{aligned} Cf_x &= \frac{2\mu_{hnf}}{\rho U^2}\left(\frac{\partial v_x}{\partial r}\right)_{r=R(x)}, Nu_x = -\frac{x\kappa_{hnf}}{T_w - T_{in}}\left(\left(\frac{\partial T}{\partial r}\right)_{r=R(x)} + q_r\right) \\ Sh_x &= -\frac{xD_{BM}}{C_w - C_{in}}\left(\frac{\partial C}{\partial r}\right)_{r=R(x)}.Nm_x = -\frac{xD_{MO}}{M_w - M_{in}}\left(\frac{\partial M}{\partial r}\right)_{r=R(x)} \end{aligned}\right\} \quad (08)$$

The continuity Eq. in (02) is satisfied for the above-mentioned transformation and the transformed systems of equations are

$$\left.\begin{aligned}
&2\frac{\mu_{hnf}}{\mu_{bf}}\left(1+\beta^{-1}\right)\left(\xi f''\right)'+\frac{\rho_{hnf}}{\rho_{bf}}ff'-\frac{\sigma_{hnf}}{\sigma_{bf}}M_F\left(f'-\delta\right)=0\\
&\frac{\kappa_{hnf}}{\kappa_{bf}}\frac{1}{Pr}\left(2+RD\right)\left(\xi\vartheta'\right)'+\frac{\left(\rho c_p\right)_{hnf}}{\left(\rho c_p\right)_{bf}}\left[f\vartheta'+2\xi\left(N_{BM}\vartheta'h'+N_{TP}\left(\vartheta'\right)^2\right)\right]=0\\
&2\left(\xi h'\right)'+Le.fh'+2\frac{N_{TP}}{N_{BM}}\left(\xi\vartheta'\right)'=0\\
&2\left(\xi m'\right)'+Pr.Lb.fm'-Pe\left[2\xi\left(m'h'+mh''+\Upsilon h''\right)+\left(m+\Upsilon\right)h\right]=0
\end{aligned}\right\}$$

(09)

The associated boundary conditions are

$$\left.\begin{aligned}
&f\left(a\right)=\frac{\varpi a}{2},\ f'\left(a\right)=\frac{\varpi}{2},\vartheta\left(a\right)=1,N_{BM}\vartheta'\left(a\right)+N_{TP}h'\left(a\right)=0,m\left(a\right)=1\\
&f'\to\frac{1-\varpi}{2},\vartheta\to 0,h\to 0,m\to 0\ as\ \xi\to\infty
\end{aligned}\right\}$$

(10)

The dimensionless parameters presented in (09-10) are

$$\left.\begin{aligned}
&M_F=\frac{\sigma B_0^2}{2\left(\rho c_p\right)_{bf}U},\delta=\frac{U_{in}}{U_w},RD=\frac{16\sigma^* T_{in}^3}{3k\kappa_{bf}\left(\rho c_p\right)_{bf}},Pr=\frac{\nu_{bf}}{\alpha_{bf}},N_{BM}=\frac{\tau D_{BM}C_{in}}{\nu_{bf}},\\
&N_{TP}=\frac{\tau D_{TP}\left(T_w-T_{in}\right)}{T_{in}\nu_{bf}},Le=\frac{\alpha_{bf}}{D_{BM}},Lb=\frac{\alpha_{bf}}{D_{MO}},Pe=\frac{bW_c}{D_{MO}},\Upsilon=\frac{M_{in}}{M_w-M_{in}},\varpi=\frac{U}{U_w}
\end{aligned}\right\}$$

(11)

Also, the reduced dimensionless physical quantities are

Skin friction $Cfr=\dfrac{\left(8a\right)^{0.5}f''\left(a\right)}{\left(1-\varphi_1\right)^{2.5}\left(1-\varphi_2\right)^{2.5}}$

Nusselt number, $Nur=-\dfrac{\kappa_{hnf}}{\kappa_{bf}}a^{0.5}\left(2+RD\right)\vartheta'\left(a\right)$

Sherwood number for nanoparticles, $Shr=-2a^{0.5}h'\left(a\right)$

Microorganism's number, $Mor=-2a^{0.5}m'\left(a\right)$

Solution Techniques:

The changed overseeing Conditions (09) alongside the limit conditions (10) are switched over completely to introductory worth issue and are tackled utilizing RKF-45 strategy with the assistance of shooting method

$$\begin{bmatrix} f & \vartheta & h & m \\ f' & \vartheta' & h' & m' \\ f'' & \vartheta'' & h'' & m'' \\ f''' & 0 & 0 & 0 \end{bmatrix} = \begin{bmatrix} d_1 & d_4 & d_6 & d_8 \\ d_2 & d_5 & d_7 & d_9 \\ d_3 & d_5' & d_7' & d_9' \\ d_3' & 0 & 0 & 0 \end{bmatrix}$$

(12)

Using the above relations, the Equations (09) are converted to first order equations as follows:

$$\begin{pmatrix} d_1' \\ d_2' \\ d_3' \\ d_4' \\ d_5' \\ d_6' \\ d_7' \\ d_8' \\ d_9' \end{pmatrix} = \begin{pmatrix} d_2 \\ d_3 \\ -\frac{1}{\xi}\left[d_3 + \frac{1}{2\frac{\mu_{hnf}}{\mu_{bf}}\left(1+\beta^{-1}\right)} \left\{ \frac{\rho_{hnf}}{\rho_{bf}} d_1 d_2 - \frac{\sigma_{hnf}}{\sigma_{bf}} M_F \left(d_2 - \delta \right) \right\} \right] \\ d_5 \\ -\frac{1}{\xi}\left[d_5 + \frac{Pr}{\left(2+RD\right)} \frac{\kappa_{bf}}{\kappa_{hnf}} \frac{\left(\rho c_p\right)_{hnf}}{\left(\rho c_p\right)_{bf}} \left\{ d_1 d_5 + 2\xi \left(N_{BM} d_5 d_7 + N_{TP} {d_5}^2 \right) \right\} \right] \\ d_7 \\ -\frac{1}{2\xi}\left\{ 2d_7 + Le.d_1 d_7 + 2\frac{N_{TP}}{N_{BM}} \left(\xi d_5' + d_5 \right) \right\} \\ d_9 \\ -\frac{1}{2\xi}\left[2d_9 + Pr.Lb.d_1 d_9 - Pe\left\{ 2\xi \left(d_7 d_9 + d_8 d_7' + \Upsilon d_7' \right) + \left(d_8 + \Upsilon \right) d_6 \right\} \right] \end{pmatrix}$$

(13)

The associated initial conditions are

$$\left.\begin{aligned} & d_1(a) = \frac{\varpi a}{2}, d_2(a) = \frac{\varpi}{2}, d_3(a) = \alpha_1, d_4(a) = 1, d_5(a) = \alpha_2, \\ & d_6(a) = \alpha_3, d_7(a) = -\frac{N_{BM}}{N_{TP}} \alpha_2, d_8(a) = 1, d_9(a) = \alpha_4 \end{aligned}\right\}$$

(14)

In the above starting worth issue, five circumstances are known and the excess $(\alpha_1, \alpha_2, \alpha_3, \alpha_4)$ still up in the air by utilizing shooting strategy. Afterward, the calculations are performed by setting $\xi = 10$ for the far field limit conditions and are addressed utilizing RKF-45 request technique with a precision of 10^{-5}. This technique decides the legitimate step size and at each step, two approximations are made and analyzed. In the event that these two approximations hold close concurrence with one another, it is acknowledged. Else, the step

size is additionally diminished and the calculation is rehashed until required exactness is accomplished. The outcome is confirmed by contrasting it and the current writing and the correlation is shown in Table 3.

Table 3: Validation of results

Pr	$\vartheta'(0.1)$		
	Qasim et al. [53]	Suleman et al. [54]	Present work
0.72	1.23664	1.23665	1.23665
1	1.0000	1.0000	1.0000
6.7	0.3333	0.33331	0.33332
10	0.26876	0.26877	0.26876

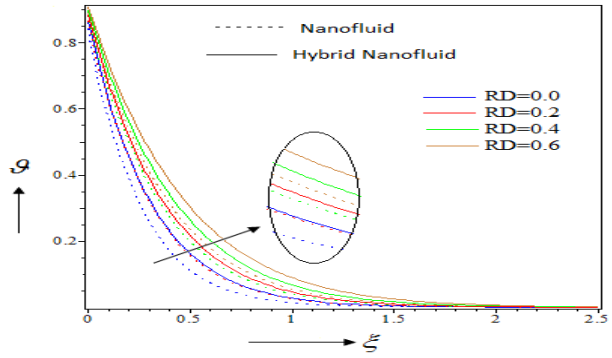

Figure 02: Effects of RD on $\vartheta(\xi)$

Result and discussions:

The mathematical calculations have been performed to investigate the impact of different boundaries on the temperature, focus and microorganism's thickness profile. The outcomes are acquired as diagrams outlines including the way of behaving of skin grinding coefficient, Nusselt number, and motile thickness number. We are centered on the examination of the outcomes between Ag/H_2O nanofluid and $Ag+TiO_2/H_2O$ hybrid nanofluid.

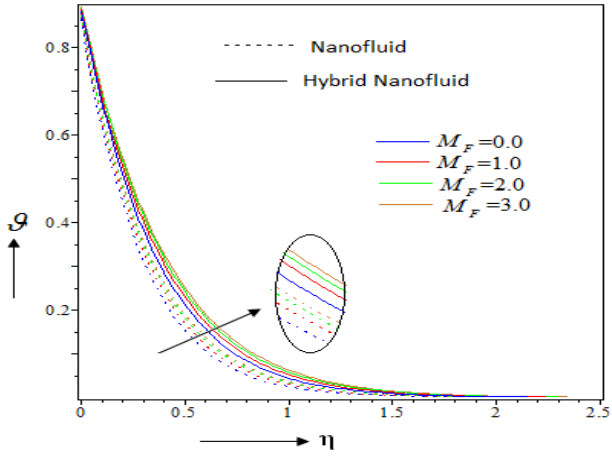

Figure 03: Effects of M_F on $\vartheta(\xi)$

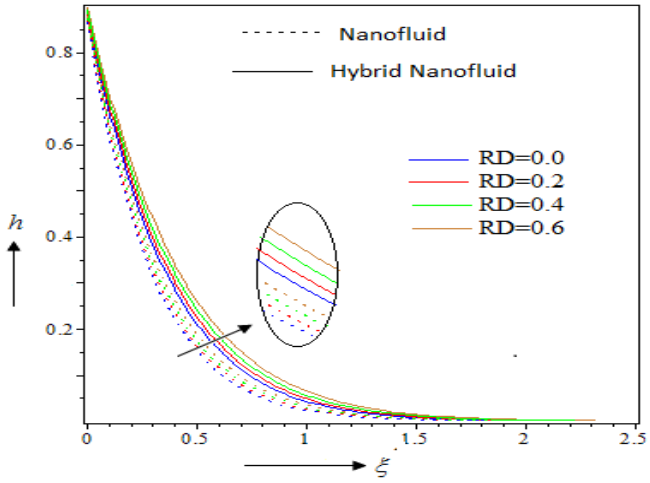

Figure 04: Effects of RD on $h(\xi)$

First, we examine about the impacts of radiation boundary on the temperature of the progression of nanofluid and cross breed nanofluid. As displayed in figure 02, we witness that high radiation in the stream brings about rise in the temperature of the stream.

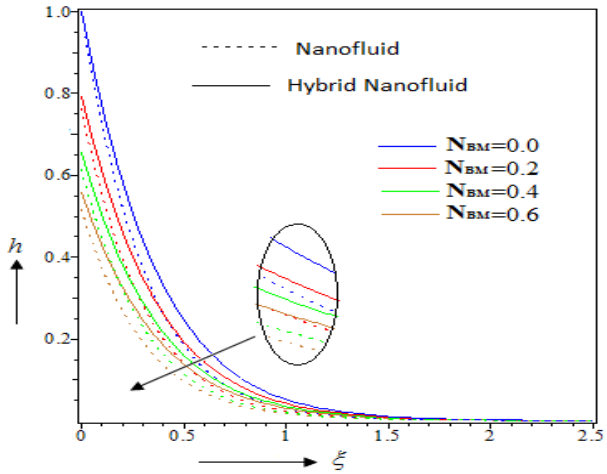

Figure 05: Effects of N_{BM} on $h(\xi)$

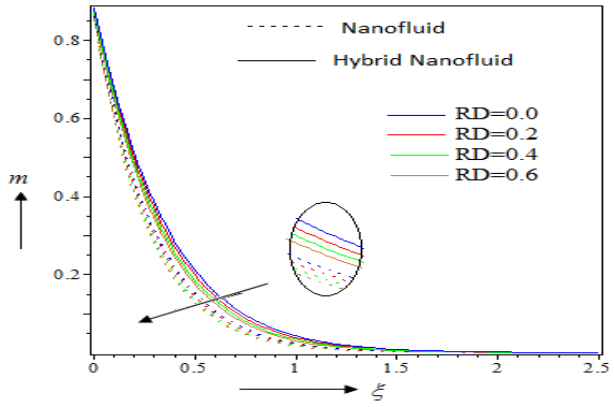

Figure 06: Effects of RD on $m(\xi)$

However, it is worth focusing on that in the event of half breed nanofluid stream it answers more noticeably to the radiation than that of nanofluid stream. Additionally, with the higher separation from the outer layer of the stream, the temperature of the stream framework steadily and reliably diminishes to nothing. Comparable impact is seen in the event of impact of attractive boundary on the temperature of the stream in figure 03. Here we witness that higher attractive power implies higher Lorentz force that impedes the progression of the liquid which gives the nanoparticles to retain additional intensity energy from the stream surface and in this way, it expands the temperature of the stream. We likewise witness that mixture nanoparticles are more effectively equipped for engrossing intensity than nanoparticle. The impact of radiation on the nanoparticle thickness is organized I figure 04. It is perceptibly upgraded with higher radiation close to the outer layer of the stream.

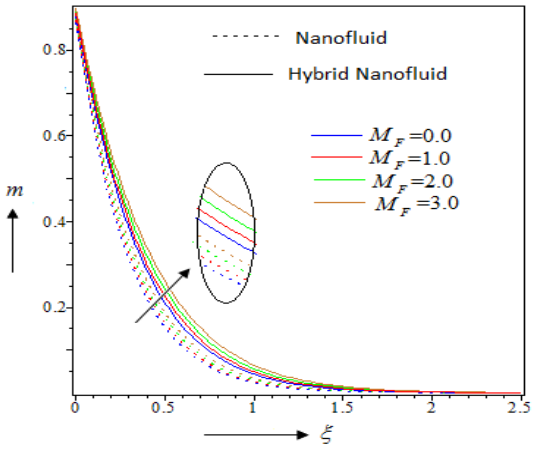

Figure 07: Effects of M_F on $m(\xi)$

Additionally, we are keen on working out the impacts of Brownian movement factor on the nanoparticle thickness as introduced in figure 05. Here it is fascinating to see that raised arbitrary development of the nanoparticle reduces the nanoparticle thickness close to the surface, yet in the event of half and half nanofluid its thickness diminishes less. In figure 06-07, how is the microorganism thickness affected by the radiation and attractive power? At the point when we increment the radiation in the outer layer of the stream, we see that microorganisms are swimming away from the surface because of the expanded temperature in the stream. Be that as it may, it is getting increasingly dense if there should arise an occurrence of higher attractive power field.

Table 04: Values of physical quantities subject to the various factors

RD	M_F	*Cfr*		*Nur*		*Shr*		*Mor*	
		Ag/ H_2O	Ag+Ti O_2/ H_2O	Ag/ H_2O	Ag+Ti O_2/ H_2O	Ag/ H_2O	Ag+Ti O_2/ H_2O	Ag/ H_2O	Ag+Ti O_2/ H_2O
0.0	1.0	0.124536	0.102345	7.501215	8.611254	2.456589	2.699871	0.822359	1.335473

0.1		0.234415	0.217845	6.998548	8.120245	2.211547	2.522130	1.022358	1.640012
0.2		0.354568	0.345156	6.500568	7.588941	2.012456	2.294578	1.233456	1.822457
0.3		0.445781	0.441215	5.955648	7.025480	1.800234	2.012457	1.414567	2.100245
0.4		0.562314	0.558978	5.421665	6.523012	1.700254	1.855648	1.65478	2.388457
0.2	0.0	0.361247	0.360012	4.901257	5.811248	0.122345	0.522135	1.855791	2.014789
	0.5	0.347784	0.341542	5.622315	6.455218	0.645791	1.244518	1.544781	1.911012
	1.0	0.354568	0.345156	6.500568	7.588941	2.012456	2.294578	1.233456	1.822457
	1.5	0.334518	0.330012	7.001245	8.124580	3.511249	3.800124	1.044215	1.644578
	2.0	0.301245	0.300008	7.611487	8.897513	4.945487	5.266489	0.812254	1.500248

The impacts of radiation and attractive power on the actual amounts of the stream in organized in table 04. The radiation expands the skin rubbing of the stream, which brings about lessened intensity and mass exchange of the nanoparticle. However, if there should arise an occurrence of microorganism move rate, it lifts with higher radiation. Additionally, because of less skin grating in half breed nanofluid stream, intensity and mass exchange rate is a lot higher than that of nanofluid stream. With regards to the attractive power impact on the stream, it decreases the skin erosion of the stream thus the intensity and mass exchange rate is raised with more grounded attractive field in the stream. Be that as it may, microorganism move rate is decreased with an ever-increasing number of attractive fields.

Concluding Remarks:

After cautiously noticing the bioconvective Casson stream of crossover nanofluid with gyrotactic microorganisms over flimsy slendering needle, we came to the accompanying perceptions.

1. Radiation in the stream builds the temperature of the stream as well as the intensity and mass exchange capacity of the stream. Be that as it may, in the event of cross breed nanofluid stream the impact is a lot more grounded.
2. Externally applied attractive power field raised the temperature and the mass of microorganisms. Yet, the impact on nanoparticle thickness is unimportant.
3. The skin contact of the stream is less when applied attractive power field is more grounded. That is the reason intensity and mass exchange for nanoparticle is a lot higher with more grounded attractive power.
4. The mass exchange pace of microorganisms displayed inverse patterns in both the instance of radiation and attractive field.

5. The exhibitions of crossover nanofluid in the event of intensity and mass exchange are more unmistakable than the presentation of nanofluid stream.

References:

[1] Platt JR. " bioconvection patterns" in cultures of free-swimming organisms. Science. 1961 Jun 2;133(3466):1766-7.

[2] Ghorai S, Hill NA. Wavelengths of gyrotactic plumes in bioconvection. Bulletin of mathematical biology. 2000 May;62(3):429-50.

[3] Choi SU, Jeffrey A. Eastman, enhancing thermal conductivity of fluids with nanoparticles. InASME international mechanical engineering congress & exposition 1995 Nov (pp. 12-17).

[4] Xuan Y, Roetzel W. Conceptions for heat transfer correlation of nanofluids. International Journal of heat and Mass transfer. 2000 Oct 1;43(19):3701-7.

[5] Xuan Y, Li Q. Heat transfer enhancement of nanofluids. International Journal of heat and fluid flow. 2000 Feb 1;21(1):58-64.

[6] Sinha A, Misra JC. Effect of induced magnetic field on magnetohydrodynamic stagnation point flow and heat transfer on a stretching sheet. Journal of Heat Transfer. 2014 Nov 1;136(11).

[7] Basir MF, Uddin M, Ismail A. Unsteady magnetoconvective flow of bionanofluid with zero mass flux boundary condition. Sains Malaysiana. 2017 Feb 1;46(2):327-33.

[8] Reddy NB, Poornima T, Sreenivasulu P. Radiative heat transfer effect on MHD slip flow of Dissipating Nanofluid past an exponential stretching porous sheet. Int. J. Pure Appl. Math. 2016;109(9):134-42.

[9] Sreenivasulu P, Poornima T, Bhaskar Reddy N. Thermal radiation effects on MHD boundary layer slip flow past a permeable exponential stretching sheet in the presence of joule heating and viscous dissipation. Journal of Applied Fluid Mechanics. 2015 Dec 1;9(1):267-78.

[10] Parida SK, Panda S, Rout BR. MHD boundary layer slip flow and radiative nonlinear heat transfer over a flat plate with variable fluid properties and thermophoresis. Alexandria Engineering Journal. 2015 Dec 1;54(4):941-53.

[11] Nayak MK, Shaw S, Chamkha AJ. Impact of variable magnetic field and convective boundary condition on a stretched 3D radiative flow of Cu-H2O nanofluid. AMSE JOURNALS-AMSE IIETA Series: Modelling B. 2018;86(3):658-78.

[12] Nayak MK, Akbar NS, Tripathi D, Pandey VS. Three dimensional MHD flow of nanofluid over an exponential porous stretching sheet with convective boundary conditions. Thermal Science and Engineering Progress. 2017 Sep 1;3:133-40.

[13] Das S, Sensharma A, Jana RN, Sharma RP. Slip flow of nanofluid past a vertical plate with ramped wall temperature considering thermal radiation. Journal of Nanofluids. 2017 Dec 1;6(6):1054-64.

[14] Kuznetsov AV. The onset of bioconvection in a suspension of gyrotactic microorganisms in a fluid layer of finite depth heated from below. International Communications in Heat and Mass Transfer. 2005 Apr 1;32(5):574-82.

[15] Kuznetsov AV. Thermo-bioconvection in a suspension of oxytactic bacteria. International communications in heat and mass transfer. 2005 Aug 1;32(8):991-9.

[16] Kuznetsov AV. Investigation of the onset of thermo-bioconvection in a suspension of oxytactic microorganisms in a shallow fluid layer heated from below. Theoretical and Computational Fluid Dynamics. 2005 Oct;19(4):287-99.
[17] Kuznetsov AV. The onset of thermo-bioconvection in a shallow fluid saturated porous layer heated from below in a suspension of oxytactic microorganisms. European Journal of Mechanics-B/Fluids. 2006 Mar 1;25(2):223-33.
[18] Aziz A, Khan WA, Pop I. Free convection boundary layer flow past a horizontal flat plate embedded in porous medium filled by nanofluid containing gyrotactic microorganisms. International Journal of Thermal Sciences. 2012 Jun 1;56:48-57.
[19] Tham L, Nazar R, Pop I. Mixed convection flow over a solid sphere embedded in a porous medium filled by a nanofluid containing gyrotactic microorganisms. International Journal of Heat and Mass Transfer. 2013 Jul 1;62:647-60.
[20] Tham L, Nazar R, Pop I. Steady mixed convection flow on a horizontal circular cylinder embedded in a porous medium filled by a nanofluid containing gyrotactic micro-organisms. Journal of heat transfer. 2013 Oct 1;135(10).
[21] Shaw S, Kameswaran PK, Narayana M, Sibanda P. Bioconvection in a non-Darcy porous medium saturated with a nanofluid and oxytactic micro-organisms. International Journal of Biomathematics. 2014 Jan 13;7(01):1450005.
[22] Balla CS, Haritha C, Naikoti K, Rashad AM. Bioconvection in nanofluid-saturated porous square cavity containing oxytactic microorganisms. International Journal of Numerical Methods for Heat & Fluid Flow. 2018 Nov 27.
[23] Sheremet MA, Pop I. Thermo-bioconvection in a square porous cavity filled by oxytactic microorganisms. Transport in Porous Media. 2014 Jun;103(2):191-205.
[24] Khan WA, Makinde OD. MHD nanofluid bioconvection due to gyrotactic microorganisms over a convectively heat stretching sheet. International Journal of Thermal Sciences. 2014 Jul 1;81:118-24.
[25] Khan WA, Makinde OD, Khan ZH. MHD boundary layer flow of a nanofluid containing gyrotactic microorganisms past a vertical plate with Navier slip. International journal of heat and mass transfer. 2014 Jul 1;74:285-91.
[26] Gireesha BJ, Kumar KG, Manjunatha S. Impact of chemical reaction on MHD 3D flow of a nanofluid containing gyrotactic microorganism in the presence of uniform heat source/sink. International Journal of Chemical Reactor Engineering. 2018 Dec 1;16(12).
[27] Gireesha BJ, Kumar KG, Rudraswamy NG, Manjunatha S. Effect of viscous dissipation on three dimensional flow of a nanofluid by considering a gyrotactic microorganism in the presence of convective condition. InDefect and Diffusion Forum 2018 (Vol. 388, pp. 114-123). Trans Tech Publications Ltd.
[28] Hayat T, Nadeem S. Heat transfer enhancement with Ag–CuO/water hybrid nanofluid. Results in physics. 2017 Jan 1;7:2317-24.
[29] Tayebi T, Chamkha AJ. Entropy generation analysis due to MHD natural convection flow in a cavity occupied with hybrid nanofluid and equipped with a conducting hollow cylinder. Journal of Thermal analysis and Calorimetry. 2020 Feb;139(3):2165-79.
[30] Ghalambaz M, Doostani A, Izadpanahi E, Chamkha AJ. Conjugate natural convection

flow of Ag–MgO/water hybrid nanofluid in a square cavity. Journal of Thermal Analysis and Calorimetry. 2020 Feb;139(3):2321-36.

[31] Dogonchi AS, Nayak MK, Karimi N, Chamkha AJ, Ganji DD. Numerical simulation of hydrothermal features of Cu–H2O nanofluid natural convection within a porous annulus considering diverse configurations of heater. Journal of Thermal Analysis and Calorimetry. 2020 Sep;141(5):2109-25.

[32] Manjunatha S, Kuttan BA, Jayanthi S, Chamkha A, Gireesha BJ. Heat transfer enhancement in the boundary layer flow of hybrid nanofluids due to variable viscosity and natural convection. Heliyon. 2019 Apr 1;5(4):e01469.

[33] Animasaun IL. Dynamics of unsteady MHD convective flow with thermophoresis of particles and variable thermo-physical properties past a vertical surface moving through binary mixture. Open Journal of Fluid Dynamics. 2015;5(02):106.

[34] Animasaun IL. Effects of thermophoresis, variable viscosity and thermal conductivity on free convective heat and mass transfer of non-darcian MHD dissipative Casson fluid flow with suction and nth order of chemical reaction. Journal of the Nigerian Mathematical Society. 2015 Apr 1;34(1):11-31.

[35] Sandeep N, Koriko OK, Animasaun IL. Modified kinematic viscosity model for 3D-Casson fluid flow within boundary layer formed on a surface at absolute zero. Journal of Molecular Liquids. 2016 Sep 1;221:1197-206.

[36] Chaudhary MA, Merkin JH. A simple isothermal model for homogeneous-heterogeneous reactions in boundary-layer flow. I Equal diffusivities. Fluid dynamics research. 1995 Nov 1;16(6):311-33.

[37] Chaudhary MA, Merkin JH. A simple isothermal model for homogeneous-heterogeneous reactions in boundary-layer flow. II Different diffusivities for reactant and autocatalyst. Fluid dynamics research. 1995 Nov 30;16(6):335.

[38] Makinde OD, Animasaun IL. Bioconvection in MHD nanofluid flow with nonlinear thermal radiation and quartic autocatalysis chemical reaction past an upper surface of a paraboloid of revolution. International Journal of Thermal Sciences. 2016 Nov 1;109:159-71.

[39] Lee LL. Boundary layer over a thin needle. The physics of fluids. 1967 Apr;10(4):820-2.

[40] Narain JP, Uberoi MS. Combined forced and free-convection heat transfer from vertical thin needles in a uniform stream. The Physics of Fluids. 1972 Nov;15(11):1879-82.

[41] Narain JP, Uberoi MS. Combined forced and free-convection over thin needles. International Journal of Heat and Mass Transfer. 1973 Aug 1;16(8):1505-12.

[42] Chen JL, Smith TN. Forced convection heat transfer from nonisothermal thin needles, (1978): 358-362.

[43] Ishak A, Nazar R, Pop I. Boundary layer flow over a continuously moving thin needle in a parallel free stream. Chinese Physics Letters. 2007 Oct 1;24(10):2895.

[44] Ahmad S, Arifin NM, Nazar R, Pop I. Mixed convection boundary layer flow along vertical thin needles: Assisting and opposing flows. International Communications in Heat and Mass Transfer. 2008 Feb 1;35(2):157-62.

[45] Grosan T, Pop I. Forced convection boundary layer flow past nonisothermal thin needles in nanofluids. Journal of heat transfer. 2011 May 1;133(5).

[46] Hayat T, Khan MI, Farooq M, Yasmeen T, Alsaedi A. Water-carbon nanofluid flow with variable heat flux by a thin needle. Journal of Molecular Liquids. 2016 Dec 1;224:786-91.

[47] Sung-Suh HM, Choi JR, Hah HJ, Koo SM, Bae YC. Comparison of Ag deposition effects on the photocatalytic activity of nanoparticulate TiO2 under visible and UV light irradiation. Journal of Photochemistry and Photobiology A: Chemistry. 2004 Apr 15;163(1-2):37-44.

[48] Sclafani A, Herrmann JM. Influence of metallic silver and of platinum-silver bimetallic deposits on the photocatalytic activity of titania (anatase and rutile) in organic and aqueous media. Journal of Photochemistry and Photobiology A: Chemistry. 1998 Feb 28;113(2):181-8.

[49] Yin S, Hasegawa H, Maeda D, Ishitsuka M, Sato T. Synthesis of visible-light-active nanosize rutile titania photocatalyst by low temperature dissolution–reprecipitation process. Journal of Photochemistry and Photobiology A: Chemistry. 2004 Apr 15;163(1-2):1-8.

[50] Amirsom NA, Uddin MJ, Ismail AI. MHD boundary layer bionanoconvective non-Newtonian flow past a needle with Stefan blowing. Heat Transfer—Asian Research. 2019 Mar;48(2):727-43.

[51] Rosseland S. Astrophysik: Auf atomtheoretischer grundlage. Springer-Verlag; 2013 Nov 22.

[52] Tian XY, Li BW, Zhang JK. The effects of radiation optical properties on the unsteady 2D boundary layer MHD flow and heat transfer over a stretching plate. International Journal of Heat and Mass Transfer. 2017 Feb 1;105:109-23.

[53] Qasim M, Khan ZH, Khan WA, Ali Shah I. MHD boundary layer slip flow and heat transfer of ferrofluid along a stretching cylinder with prescribed heat flux. PloS one. 2014 Jan 22;9(1):e83930.

[54] Suleman M, Ramzan M, Ahmad S, Lu D, Muhammad T, Chung JD. A numerical simulation of silver–water nanofluid flow with impacts of newtonian heating and homogeneous–heterogeneous reactions past a nonlinear stretched cylinder. Symmetry. 2019 Feb 24;11(2):295.